BENCHMARKS FOR VERIFICATION OF HEDP/IFE CODES

Ryan G. McClarren, Daniel Holladay
Department of Nuclear Engineering,Texas A&M University, College Station, TX 77843
rgm@tamu.edu, dholladay00@neo.tamu.edu

We present the first semi-analytic radiation transport solutions for the three-temperature (3-T) model: the equations that couple radiation, electron, and ion energy density in a dense plasma. The problem we solve is the 3-T version of the Su-Olson problem considered in a recent radiation diffusion study for verification of a production HEDP code. After linearizing the equations, integral transforms are used to solve the equations, and the inverse transforms are computed numerically after considerable simplication. The results are compared to 2-T transport and 3-T diffusion solutions.

I INTRODUCTION

An indispensible aspect of building confidence in simulation codes is the demonstration that the code solves the equations/mathematical model correctly. This exercise is known as code verification. An important part of code verification is the comparison between numerical results and analytic solutions to demonstrate that the code converges at the appropriate rate. Code verification for multiphysics simulations is complicated by the dearth of analytic solutions to the nonlinear, coupled partial differential equations that comprise these simulations. This work develops verification solutions for a specific aspect of plasma simulation, the coupling of radiation, electron, and ion energies, in inertial fusion energy (IFE) and high-energy-density physics (HEDP) applications. The model we solve is known as the 3-T equations and will be detailed in the next section.

The problem that we solve was originally defined by McClarren and Wöhlbier[1], in a recent paper. That work considered a diffusion model for the transport of radiation; here we extend that work by dispensing with the diffusion model and use a full-fidelity, gray, radiation transport model. The problem solved is also an extension to the linearized problems that assume equilbrium between electrons and ions solved by Su and Olson under several regimes of approximation: gray diffusion[2], gray transport[3], and multifrequency diffusion and transport[4]. This problem linearizes the equations for radiation-material coupling in order to obtain analytic solutions. Despite the fact that the linearization uses a nonphysical form for the heat capacity, the Su-Olson solutions have obtained routine use in verifying HEDP codes (the three papers mentioned above have been cited over 80 times). For the 3-T equations, the previously presented diffusion solutions have been used to verify production codes[1,5], and it is our expectation that the transport solutions will be similarly useful.

II THE 3-T MODEL

The three-temperature (3-T) equations[6,7] describe a plasma system with distinct ion and electron temperatures where the presence of radiation can significantly affect the system's evolution. The equations that we consider treat the radiation energy using a transport description under the gray approximation and model the electron and ion transport processes using a diffusion process. We also assume that hydrodynamic effects, as well as electric and magnetic field effects, are split from the energy balance equations. The equation for the radiation intensity in a one-dimensional slab is[8]

$$\frac{1}{c}\frac{\partial I}{\partial \tau}+\mu\frac{\partial I}{\partial z}+\sigma I=\frac{\sigma acT_{\mathrm{e}}^4}{2}+\frac{S_{\mathrm{r}}}{2}. \qquad (1)$$

Here $I(z,\mu,\tau)$ is the specific intensity of radiation with units of energy/(area $\cdot$ time), where z is the distance in the normal direction to the slab, $\mu\in[-1,1]$ is the cosine of the angle between the slab normal and a direction of radiation propagation, and τ is time. The radiation interacts with the material medium through absorption processes and σ is the absorption opacity with units of inverse length, $T_{\mathrm{e}}(z,\tau)$ is the electron temperature, c is the speed of light, $a=4\sigma_{\mathrm{SB}}/c$ is the radiation constant defined in terms of the Stefan-Boltzmann constant, σ_{SB}. The isotropically emitting radiation source is $S_{\mathrm{r}}(x,t)$. The electron energy density, $e_{\mathrm{e}}(x,t)$, is governed by an equation that takes

into account the exchange of energy between radiation and electrons and between electrons and ions as well as the diffusion of electron energy by heat conduction:

$$\frac{\partial e_\mathrm{e}}{\partial \tau} = \frac{\partial}{\partial z}\kappa_\mathrm{e}\frac{\partial T_\mathrm{e}}{\partial z} + \gamma_\mathrm{ei}(T_\mathrm{i} - T_\mathrm{e}) - \sigma\left(acT_\mathrm{e}^4 - \varphi\right) + S_\mathrm{e}, \tag{2}$$

where the scalar intensity is defined as $\varphi = \int_{-1}^{1} I\, d\mu$, κ_e is the electron diffusion coefficient, γ_ei is the electron-ion coupling coefficient, and $S_\mathrm{e}(x,t)$ is the electron energy source. Similarly, the ion internal energy density, $e_\mathrm{i}(x,t)$, is governed by

$$\frac{\partial e_\mathrm{i}}{\partial \tau} = \frac{\partial}{\partial z}\kappa_\mathrm{i}\frac{\partial T_\mathrm{i}}{\partial z} - \gamma_\mathrm{ei}(T_\mathrm{i} - T_\mathrm{e}) + S_\mathrm{i}, \tag{3}$$

with κ_i the ion diffusion coefficient, and $S_\mathrm{i}(x,t)$ the ion energy source. The heat capacity,

$$C_{\mathrm{v}\alpha} = \frac{\partial e_\alpha}{\partial T_\alpha}, \quad \alpha = \mathrm{e}, \mathrm{i}, \tag{4}$$

relates the internal energy density to the species temperature via an equation of state assuming a stationary material. This leads to

$$\frac{\partial e_\alpha}{\partial \tau} = C_{\mathrm{v}\alpha}\frac{\partial T_\alpha}{\partial t}, \quad \alpha = \mathrm{e}, \mathrm{i}. \tag{5}$$

II.A Linearization

As initially introduced in[1] we prescribe forms for several material parameters. These forms *are not* necessarily physically realistic: they are chosen so that the equations are soluble. The solutions we obtain will be used to test computer codes, which generally have the flexibility to treat general forms of these parameters. Specifically we set the heat capacity to be proportional to the species temperature to the third power: $C_{\mathrm{v}\alpha} = 4aT_\alpha^3$. This form for the specific heat was first introduced for the two-temperature case by Pomraning[9]. This makes the energy density for each species

$$e_\alpha = \int_0^{T_\alpha} C_{\mathrm{v}\alpha}(T)\, dT = aT_\alpha^4 \tag{6}$$

For the 3-T equations we must introduce other linearizations; specifically, we set the heat conduction coefficients to $\kappa_\alpha = 4a\bar{\kappa}_\alpha T_\alpha^3$, and the electron-ion coupling coefficient to

$$\gamma_\mathrm{ei} = a\bar{\gamma}\frac{T_\mathrm{i}^4 - T_\mathrm{e}^4}{T_\mathrm{i} - T_\mathrm{e}}. \tag{7}$$

Using these forms for material parameters, the 3-T equations become the linear system of equations

$$\frac{1}{c}\frac{\partial I}{\partial \tau} + \mu\frac{\partial I}{\partial z} + \sigma I = \frac{c\sigma e_\mathrm{e}}{2} + \frac{S_\mathrm{r}}{2}, \tag{8a}$$

$$\frac{\partial e_\mathrm{e}}{\partial \tau} = \bar{\kappa_\mathrm{e}}\frac{\partial^2 e_\mathrm{e}}{\partial z^2} + \bar{\gamma}(e_\mathrm{i} - e_\mathrm{e}) - \sigma\left(ce_\mathrm{e} - \varphi\right) + S_\mathrm{e}, \tag{8b}$$

and

$$\frac{\partial e_\mathrm{i}}{\partial \tau} = \bar{\kappa_\mathrm{i}}\frac{\partial^2 e_\mathrm{i}}{\partial z^2} - \bar{\gamma}(e_\mathrm{i} - e_\mathrm{e}) + S_\mathrm{i}, \tag{8c}$$

where we have also assumed that the κ_α's are spatially constant.

II.B Non-dimensionalization

To non-dimensionalize the linearized 3-T equations we first introduce a reference temperature T_H, called the hohlraum temperature, and then introduce the following non-dimensional variables

$$t = c\sigma\tau, \qquad x = \sigma z, \qquad \psi = \frac{I}{acT_\mathrm{H}^4},$$
$$U_\mathrm{i} = \frac{e_\mathrm{i}}{aT_\mathrm{H}^4}, \qquad U_\mathrm{e} = \frac{e_\mathrm{e}}{aT_\mathrm{H}^4}, \qquad \phi = \frac{\varphi}{acT_\mathrm{H}^4},$$
$$D_\mathrm{i} = \frac{\bar{\kappa_\mathrm{i}}\sigma}{c}, \qquad D_\mathrm{e} = \frac{\bar{\kappa_\mathrm{e}}\sigma}{c}, \qquad \gamma = \frac{\bar{\gamma}}{c\sigma},$$
$$Q_\mathrm{e} = \frac{S_\mathrm{e}}{\sigma acT_\mathrm{H}^4}, \qquad Q_\mathrm{i} = \frac{S_\mathrm{i}}{\sigma acT_\mathrm{H}^4}, \qquad Q_\mathrm{r} = \frac{S_\mathrm{r}}{\sigma acT_\mathrm{H}^4}.$$

Using these definitions Eqs. (8) become the non-dimensional equations

$$\frac{\partial \psi}{\partial t} + \mu\frac{\partial \psi}{\partial x} + \psi = \frac{U_\mathrm{e}}{2} + \frac{Q_\mathrm{r}}{2}, \tag{9a}$$

$$\frac{\partial U_\mathrm{e}}{\partial t} = D_\mathrm{e}\frac{\partial^2 U_\mathrm{e}}{\partial z^2} + \gamma(U_\mathrm{i} - U_\mathrm{e}) - (U_\mathrm{e} - \phi) + Q_\mathrm{e}, \tag{9b}$$

and

$$\frac{\partial U_\mathrm{i}}{\partial t} = D_\mathrm{i}\frac{\partial^2 U_\mathrm{i}}{\partial z^2} - \gamma(U_\mathrm{i} - U_\mathrm{e}) + Q_\mathrm{i}. \tag{9c}$$

These are the equations that we will solve.

III PROBLEM

We consider and infinite medium with conditions such that at $x = \pm\infty$ the solutions for ψ, U_e, and U_i vanish. Additionally, the initial conditions are such that there is no energy in any species initially:

$$\psi(x,\mu,0) = 0, \qquad U_\mathrm{e}(x,0) = 0, \qquad U_\mathrm{i}(x,0) = 0. \tag{10}$$

The sources in the electron and ion equations are set to zero everywhere, and there is a finite radiation source: $Q_\mathrm{e} = 0$, $Q_\mathrm{i} = 0$, and

$$Q_\mathrm{r} = \begin{cases} \frac{1}{2x_0}\left(\mathrm{H}(x+x_0) - \mathrm{H}(x-x_0)\right) & 0 \le t \le t_0 \\ 0 & t > 10 \end{cases}, \tag{11}$$

where $H(x)$ is the Heaviside step function.

We now perform Laplace and Fourier transforms of the linear, nondimensional 3-T equations. The convention we use for these transforms is

$$\hat{u}(k,s) = \int_0^\infty dt \int_{-\infty}^\infty dx\, u(x,t) e^{-(ikx+st)}, \tag{12}$$

and the inverse transforms are given by

$$u(x,t) = \frac{-i}{(2\pi)^2} \int_{\rho-i\infty}^{\rho+i\infty} ds \int_{-\infty}^{\infty} dk\, \hat{u}(k,s) e^{(ikx+st)}, \tag{13}$$

where the inverse Laplace transform's integration is over the usual Bromwich contour with ρ a real number chosen so that the contour is to the right of all singularities in the complex plane. Upon Laplace and Fourier transforming Eqs. (9) and using Eqs. (10)-(11) we get

$$s\hat{\psi} + \mu i k \hat{\psi} + \hat{\psi} = \frac{\hat{U}_\mathrm{e}}{2} + \frac{\hat{Q}_\mathrm{r}}{2}, \tag{14a}$$

$$s\hat{U}_\mathrm{e} = -D_\mathrm{e} k^2 \hat{U}_\mathrm{e} + \gamma(\hat{U}_\mathrm{i} - \hat{U}_\mathrm{e}) - \left(\hat{U}_\mathrm{e} - \hat{\phi}\right), \tag{14b}$$

and

$$s\hat{U}_\mathrm{i} = -D_\mathrm{i} k^2 U_\mathrm{i} - \gamma(\hat{U}_\mathrm{i} - \hat{U}_\mathrm{e}), \tag{14c}$$

with $\hat{Q}_\mathrm{r}$ defined by performing the integral transforms on Q_r Equation (14a) can be rearranged into the equation $\hat{\phi} = b(k,s)\left(\hat{U}_\mathrm{e} + \hat{Q}_\mathrm{r}\right)$, by defining the singular integral function

$$b(k,s) = \frac{1}{2}\int_{-1}^{1} \frac{d\mu}{1+s+\mu i k}. \tag{15}$$

Solving Eqs. (14b), (14c), and the equation for $\hat{\phi}$ gives the transformed value of the independent functions. The solution for $\hat{\phi}$ is

$$\hat{\phi} = b(k,s)\hat{Q}_\mathrm{r} - \frac{b(k,s)^2 \hat{Q}_\mathrm{r}\left(D_\mathrm{i}k^2 + s + \gamma\right)}{\gamma^2 - \left(D_\mathrm{i}k^2 + s + \gamma\right)\left(-b(k,s) + D_\mathrm{e}k^2 + s + \gamma + 1\right)}. \tag{16}$$

The solutions for $\hat{U}_\mathrm{e}$ and $\hat{U}_\mathrm{i}$ have similar forms.

To perform the inverse transforms we must determine the poles of the transformed solutions in order to properly determine the Bromwich contour. Examining the denominators of Eq. (16) we see that the poles occur where

$$b(k,s) = \frac{\gamma\left(k^2(D_\mathrm{e}+D_\mathrm{i}) + 2s + 1\right)}{D_\mathrm{i}k^2 + s + \gamma} + \frac{\left(D_\mathrm{e}k^2 + s + 1\right)\left(D_\mathrm{i}k^2 + s\right)}{D_\mathrm{i}k^2 + s + \gamma}. \tag{17}$$

We can prove that Eq. (17) is only satisfied if $\Re(s) < 0$. To prove this we first define the RHS of Eq. (17) to be a function of k that we call $L(k)$. It is easy to show the real part of $L(k)$ is always positive because D_i, D_e, and γ are positive. Furthermore, one can show that the minimum of $|L(k)|$ is greater than one when $\Re(s) > 0$. This fact derives from the fact that $\partial_k L(k)$ has only real root, $k = 0$. This makes it possible to show $|L(k)| > 1$ when $\Re(s) > 0$ as follows. At $k = 0$

$$|L(0)| = \left|\frac{(1+s)s + (1+2s)\gamma}{s+\gamma}\right| > 1, \tag{18}$$

when $\Re(s) > 0$. Also, $\lim_{k\to\pm\infty}|L(k)| = \infty$ when $\Re(s) > 0$. Therefore, the fact that $|L(k)|$ is greater than one at $k = 0$ and as $k \to \pm\infty$ when $\Re(s) > 0$ implies that $|L(k)| > 1$ for all k when $\Re(s) > 0$. Also, $|b(k,s)| \le 1$ so that it is impossible for Eq. (17) to be satisfied when $\Re(s) > 0$, and the poles in s are all in the left-half of the complex plane.

Therefore, we can take the Bromwich contour to be the imaginary axis ($\rho = 0$), and change the inverse transforms to

$$u(x,t) = \frac{1}{(2\pi)^2} \int_{-\infty}^{\infty} d\omega \int_{-\infty}^{\infty} dk\, \hat{u}(k,\omega) e^{i(kx+\omega t)}, \tag{19}$$

using $s = i\omega$; we also redefine $b(k,s)$ using this replacement for s.

Equations (16), can be written as a sum of a real part and an imaginary part. Additionally, we can write the exponential in the inverse transforms—see Eq. (19)—as the sum of a real and imaginary part. Therefore, after some amount of simplification, we can split the inverse transforms into real and imaginary parts. The imaginary part is identically zero from physical arguments, and therefore we only have to solve for the real part. The real part can be decomposed into even and odd parity components in ω and k, and, using the fact that

the odd parity components integrate to zero, we need to compute integrals of the form

$$u(x,t) = \frac{1}{\pi^2}\int_0^\infty d\omega \int_0^\infty dk\, \mathcal{U}(k,\omega), \qquad (20)$$

where $\mathcal{U}(k,\omega)$ is the real, even parity part of the integrand in Eq. (19).

IV RESULTS

Given the simplified integrals we are in a position to compute the solution to 3-T problems. The problem we will solve is a 3-T analog to the problem solved by Su and Olson[3] by setting $x_0 = 0.5$, $t_0 = 10$. This will allow direct comparison between the 2-T results and 3-T for transport. Additionally, we set $\gamma = 0.5$, $D_\mathrm{e} = \frac{1}{6}$, and $D_\mathrm{i} = 0$ to directly compare with the diffusion solution in[1]. To compute our solution, the integrals of the form in Eq. (20) were computed using Mathematica and its `NIntegrate` function. For an integration strategy we use an open Newton-Coates rule of order 2. As a check of our integration strategy we have solved the 3-T problems with $\gamma = D_\mathrm{e} = D_\mathrm{i} = 0$ to assure that we match the solutions by Su and Olson[3].

In Fig. 1 we compare 3-T solutions to the tabulated 2-T solutions in[3]. In these figures we see several phenomena introduced by having separate ion/electron temperatures, as well as electron heat conduction. At late times there is much less energy in the radiation field in the 3-T case than the 2-T case. This is due to the fact that radiation only directly couples with the electrons in our model. Therefore, when the electrons give energy to the ions through equilibration, that energy no longer couples to the radiation. Also, the presence of electron heat conduction smooths the region around the edge of the source at $x = 0.5$: the 2-T solution for U has a steeper drop off at this point than that in the 3-T solution. This effect is much less noticeable in the radiation energy density. At early time, $t = 1$, the radiation energy density is nearly the same in both solutions. This is due to the fact that at this early time the source of radiation still dominates the emission term of radiation because the electron temperature is still small.

The differences between radiation transport and radiation diffusion on this problem are shown in Fig. 2. The main difference between the models is that the transport solution has more radiation energy near $x = 0$ than the diffusion solution. This

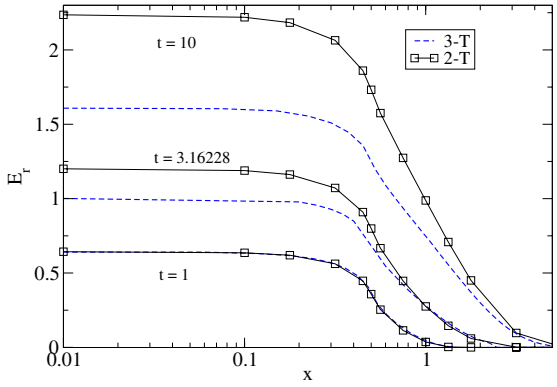

(a) Radiation Energy

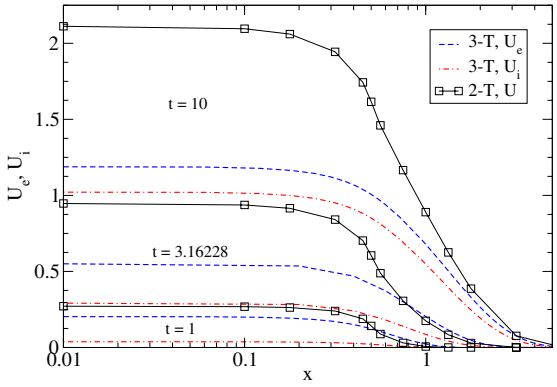

(b) Material Energy,

Figure 1: Comparison of 2-T and 3-T radiation transport solutions to the Su-Olson problem ($x_0 = 0.5$, $t_0 = 10$) on a semilog scale at times $t = 1, 3.16228, 10$. The 3-T solutions used $D_\mathrm{e} = \frac{1}{6}$, $\gamma = 0.5$, $D_\mathrm{i} = 0$.

is due to the fact that diffusion models allow radiation to flow faster than physically reasonable. This can be ameliorated by a flux-limiter; however, flux-limiting is an inherently nonlinear process and previous analytic solutions have not consider this[1]. Future work should look at how flux-limited diffusion solutions compare to the transport solutions. Another difference between the solutions is the transition from the source region, i.e., $x < 0.5$, to the region outside the source, i.e., $x > 0.5$. In the transport solution there is a noticeable transition in the shape of the solution at $x = 0.5$. The diffusion solution smears out this transition. Finally, note that at $t = 1$ the solutions for the ion energy densities are very similar as a result of there being only a small amount of coupling between the radiation, which is driving the problem, and the ion energy density at this early time.

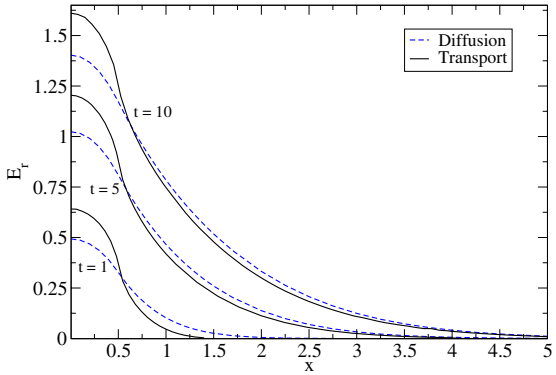

(a) Radiation Energy

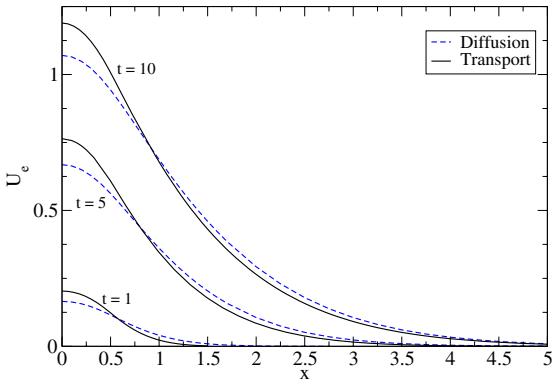

(b) Electron Energy,

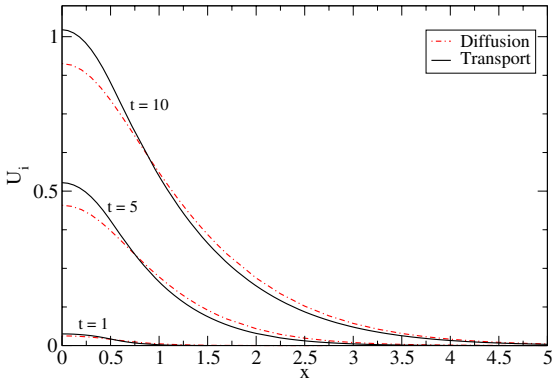

(c) Ion Energy,

Figure 2: Comparison of 3-T radiation transport and radiation diffusion solutions to the Su-Olson problem ($x_0 = 0.5$, $t_0 = 10$) at times $t = 1, 5, 10$. The solutions used $D_\mathrm{e} = \frac{1}{6}$, $\gamma = 0.5$, $D_\mathrm{i} = 0$.

V SUMMARY AND CONCLUSIONS

Above we presented the first semi-analytic solutions to the 3-T equations with radiation transport, electron/ion coupling, and heat conduction. These solutions were obtained through integral transform techniques after linearizing the equations through particular choices of material properties and simplifying the transforms. We compared the 3-T transport solutions to both 2-T transport solutions and 3-T diffusion solutions.

We believe that these solutions will be useful in testing radiation hydrodynamics codes for HEDP and IFE. Indeed, we plan on conducting comparisons to numerical results from production codes in a similar manner to[1]. Additional future work will extend these slab geometry solutions to spherical geometry.

ACKNOWLEDGMENT

This research was supported by the DOE NNSA under the Predictive Science Academic Alliance Program by grant DEFC52-08NA28616.

REFERENCES

1. R. G. MCCLARREN, J. G. WÖHLBIER, *J. Quant. Spec. Rad. Transf.* **112** (1) (2010) 119–130.

2. B. SU, G. L. OLSON, *J. Quant. Spec. Rad. Transf.* **56** (3) (1996) 337–351.

3. B. SU, G. L. OLSON, *Annals of Nuclear Energy* **24** (13) (1997) 1035–1055.

4. B. SU, G. L. OLSON, *J. Quant. Spec. Rad. Transf.* **62** (3) (1999) 279 – 302.

5. S. GOPAL, K. WEIDE, C. GRAZIANI, D. LAMB, Verification of FLASH implementations of the 3T approximation for plasma hydrodynamics, Bulletin of the American Physical Society **55** (15) (2010) 191.

6. A. M. WINSLOW, *J. Comput. Phys.* **117** (2) (1995) 262–273.

7. T. M. EVANS, J. D. DENSMORE, *J. Comput. Phys.* **225** (2) (2007) 1695–1720.

8. G. C. POMRANING, The Equations of Radiation Hydrodynamics, Dover Publications, Mineola, New York, 2005.

9. G. C. POMRANING, *J. Quant. Spec. Rad. Transf.* **21** (1979) 249–261.